Quasitopological electromagnetic response of line-node semimetals

Srinidhi T. Ramamurthy and Taylor L. Hughes

Phys. Rev. B **95**, 075138 — Published 21 February 2017

DOI: 10.1103/PhysRevB.95.075138

Quasi-Topological Electromagnetic Response of Line-node Semimetals

Srinidhi T. Ramamurthy and Taylor L. Hughes
Department of Physics, Institute for Condensed Matter Theory, University of Illinois at Urbana-Champaign, IL 61801, USA

Topological semimetals are gapless states of matter which have robust surface states and characteristic electromagnetic responses. In this paper, we consider the electromagnetic response of gapless phases in $3+1$-dimensions with line nodes. We show through a layering approach that an intrinsic antisymmetric tensor $\mathcal{B}_{\mu\nu}$ (2-form), which is determined by the geometry and energy-embedding of the nodal lines, emerges in the effective response field theory. $\mathcal{B}_{\mu\nu}$ is shown to be simply related to the charge polarization and orbital magnetization of the sample; hence the geometry of the line nodes determine these electromagnetic observables. We conclude by discussing the relevance for recently proposed materials and heterostructures with line-node fermi-surfaces.

Topological insulators (TIs) have been of great interest in recent years after their theoretical proposal and experimental discovery in the past decade. Their electronic properties led to a wide search for novel topological band structures in many materials[1, 2]. TIs are characterized by a gapped bulk and protected boundary modes that are robust in the presence of disorder. They also exhibit quantized properties in their electromagnetic (EM) response[3, 4]. A classification of non-interacting fermionic states protected by discrete time-reversal ($\mathcal{T}$), charge-conjugation ($\mathcal{C}$), and chiral symmetries has been worked out in Refs. 4–6. This has further been expanded on in recent years to include translation, reflection, and rotation symmetries of crystalline systems[7–10]. These theoretical advances have been accompanied by experimental discoveries of several TIs in various symmetry classes. The 3D $\mathcal{T}$-invariant strong TI (e.g., BiSb[11], Bi_2Se_3[12–14]), the 2D quantum spin Hall insulator (e.g., CdTe/HgTe quantum wells[15–17]), the 2D quantum anomalous Hall (Chern) insulator (e.g., Cr-doped $(Bi,Sb)_2Te_3$[3, 18]), and a 3D topological crystalline insulator (PbSnTe)[19, 20].

A defining characteristic of TIs is a gapped bulk, but one can also ask if there are gapless states of matter which harbor protected boundary modes and have unusual EM responses and transport properties. This question has been asked, and answered in the affirmative with the discovery of topological semimetals (TSMs). The most studied TSMs all have point-like Fermi surfaces, e.g., 2D Dirac semi-metals/graphene[21], 3D Weyl semimetals[22], and 3D Dirac semimetals[23, 24]. In recent work, we proposed a unifying structure to understand TSMs with point-like Fermi-surfaces, from which one can straightforwardly determine the quasi-topological EM responses[25], and which expands on previous work[26–29]. The main perspective which helps us understand these TSMs are models produced by a layering construction, and we claim that a similar idea, to be discussed below, is applicable for TSMs with line-like Fermi surfaces. Generically, a TI phase in d spatial dimensions can be layered/stacked into $d+1$ dimensions by introducing "trivial" tunneling between the layers, i.e., tunneling that does not immediately generate a $d+1$-dimensional *strong* topological phase. As the tunneling coefficient is increased, generically the material will transition from a weak topological insulator phase, which is formed in the decoupled limit, to a trivial insulating state with an intervening semimetallic gapless *phase* with point-nodes, i.e., a TSM phase. To ensure the stability of the gapless phase, additional symmetries are often required. We can extend this idea by layering a d-dimensional topological phase into $d+2$ dimensions. When the d-dimensional elements are decoupled, the $d+2$-dimensional system will be in a secondary weak topological phase characterized by an antisymmetric tensor/2-form invariant ν_{ij}[30, 31]. When the lower dimensional topological phases are coupled with strong-enough "trivial" hopping, then they will produce line-node Fermi surfaces (FLs).

The EM response of *point*-node TSMs is generally characterized by an intrinsic 1-form $b=(b_0,b_i)$ which is related to the locations of the nodes in momentum and energy space[25, 29]. The actual dependence of the EM response on b depends on the type of point-node semimetal, and can generate a wide variety of effects in 2D and 3D TSMs. We mentioned in Ref. 25 that in line-node TSM (LTSMs) phases we expect the EM response to be characterized by an analogous 2-form $B_{\mu\nu}$, which is an *intrinsic* property of the electronic structure of LTSMs that is determined by the geometry of the nodal submanifolds, and is the analog of a secondary weak invariant, though for a gapless phase. In this article we explicitly prove this to be generically true, and we find that the effective quasi-topological electromagnetic response action for LTSMs is given by

$$S[A,\mathcal{B}]=\frac{e}{16\pi^2}\int d^4x\,\epsilon^{\mu\nu\rho\sigma}\mathcal{B}_{\mu\nu}F_{\rho\sigma}. \tag{1}$$

Crucially, we show that $\mathcal{B}_{\mu\nu}$ can be determined from the geometry of the nodal Fermi surfaces in energy-momentum space. From the form of Eq. 1 we see that the components of $\mathcal{B}_{\mu\nu}$ can be related to the magnetization and polarization of the LTSM via $e\mathcal{B}_{0i}=4\pi^2 M_i$ and

$e\mathcal{B}_{ij} = 4\pi^2\epsilon_{ijk}P^k$ for $i = x, y, z$. We note that $\mathcal{B}_{\mu\nu}$ also includes components where μ, ν are in the time direction, which can be generated in a gapless system, but are not available for a time-independent gapped system. However, such components would appear in cyclically-driven gapped systems where they would take values dependent on the driving frequency.

Before we begin let us make some important comments. In this article, we only consider the EM response of 3D LTSMs with *non-degenerate* line-like Fermi surfaces. Furthermore, we only focus on a particular contribution to the response, i.e., the quasi-topological piece that is explicitly dependent on the geometry of the FLs. In contrast, we will not discuss, e.g., dissipative aspects of the LTSM EM response such as its pseudo-Ohmic conductivity, which was discussed in Ref. 32. We also make the assumption that electron-electron interactions do not destroy the quasi-particle picture of Fermi-liquid theory and, at most, renormalize the geometry of the line-node Fermi surface, and hence may create a suitably renormalized $\mathcal{B}_{\mu\nu}$. In general, interactions may destabilize the line-node to create point nodes, fully gapped systems, or when strong, may even invalidate the quasiparticle picture. We will leave questions regarding these phenomena to future work since there exist real materials for which our assumption is valid[33–35]. We also note that a version of our stacking construction for gapped phases has also been considered in Ref. 36, while a superconducting version of this, including line nodes, has been considered in [37, 38]. Additionally, in very recent work, several proposals for materials that realize line-node TSM states have appeared which utilize magnetic heterostructures[32, 39], carbon allotropes [40, 41], and inversion symmetric Cu_3PdN[42, 43]. After our primary discussion, we comment on how our analysis could be used to generate an EM response in these systems, including systems with nominally spin-degenerate FLs.

To aid our discussion it will be helpful to consider an explicit model. Although we will illustrate the EM response phenomena using a model at first, we also provide explicit general proofs that will apply to generic systems with non-degenerate FLs. Let us take the 3D Bloch Hamiltonian

$$H_3(k) = \sin k_x\sigma^y + (1+\beta+\gamma-m-\cos k_x - \beta\cos k_y - \gamma\cos k_z)\sigma^z, \quad (2)$$

which has inversion $\mathcal{I} = \sigma^z$ and time reversal $\mathcal{T} = \sigma^z K$ symmetries, where σ^a represent two (non-spin) degrees of freedom, and the lattice constant $a = 1$. When $\beta = \gamma = 0$, and $|m| \neq 1$, this model reduces to decoupled 1D insulators aligned parallel to the x-direction. Since each 1D wire is inversion symmetric, their polarizations will be quantized (and all equal). In the topological phase ($|m| < 1$), the polarization of a single wire will be $P_x(k_y, k_z) = \frac{e}{2\pi}\int \mathrm{Tr}[\mathcal{A}_x(\vec{k})]dk_x = e/2 \bmod e$[44, 45], where $\mathcal{A}_i(\vec{k})$ is the adiabatic connection matrix $\mathcal{A}_i^{ab}(\vec{k}) = -i\langle u_{a,k}|\frac{d}{dk_i}|u_{b,k}\rangle$, where a, b run over the occupied bands. If each insulator was instead in a trivial state ($|m| > 1$), we would have $P_x(k_y, k_z) = 0 \bmod e$.

In addition to the bulk topological properties, the 1D TIs have degenerate mid-gap modes localized at opposite ends of the system, the filling of which determines the bound surface charge. To unambiguously determine the sign of the bulk polarization, and hence the sign of the surface charge, one must break the degeneracy by adding an infinitesimal (inversion) symmetry breaking mass, e.g., $m_{\mathcal{I}}\sigma^y$ and take the limit as $m_{\mathcal{I}} \to 0$. Hence, for $\beta = \gamma = 0, |m| < 1$ this model represents a secondary weak TI phase protected by inversion symmetry, and the EM response is given by Eq. 1, but for the special case when $\mathcal{B}_{yz} = \mathrm{sgn}\, m_{\mathcal{I}}(\frac{1}{2}\mathbf{G}_y \wedge \mathbf{G}_z) \implies P_x = \mathrm{sgn}\, m_{\mathcal{I}}\frac{e}{2a_y a_z}$.

Now, we can find a simple example of a gapless phase if $\gamma = 0$ and β is increased until we effectively create layers of 2D Dirac semimetals. This gapless system will have two gapless lines in the Brillouin zone (BZ) at $k_y^{\pm} = \pm\cos^{-1}\frac{\beta-m}{\beta}$ for each value of k_z. These FLs are locally stable in the BZ as long as the composite $\mathcal{TI}$-symmetry is preserved. The response is given by Eq. 1 with $\mathcal{B} = \mathrm{sgn}\, m_{\mathcal{I}}(b_y \wedge \mathbf{G}_z)$ where $2b_y = k_y^+ - k_y^-$, and is a special case of our general results. We could also reverse the role of β and γ and find a phase with $\mathcal{B} = \mathrm{sgn}\, m_{\mathcal{I}}(\mathbf{G}_y \wedge b_z)$ instead.

Now let us consider a more generic/isotropic case by increasing the tunneling strengths γ, β large enough so that the insulating gap closes and a single closed FL inside the BZ forms. Performing an expansion around the origin, gaplessness will imply the constraints $k_x = 0, \pi$ and $\beta k_y^2 + \gamma k_z^2 = 2m$, i.e., the equation for an ellipse. Assuming that $\beta, \gamma > 0$ to be explicit, this constraint only has a solution when $m > 0$. Now to be concrete, we expand the Hamiltonian by assuming $\beta = \gamma = 2m = 2$ so that there is a only a single FL circle located in the $k_x = 0$ plane, and none at $k_x = \pi$. It is convenient to switch to cylindrical coordinates: $(k_x, k_y, k_z) \to (k_x, \kappa, \theta)$ where θ winds around the FL, and κ represents the (signed) radial distance *away* from the FL in the $k_y k_z$-plane. Using this definition, $(k_x = 0, \kappa = 0, \theta)$ lies on the FL and we find the Hamiltonian near the FL is

$$H_{FL}(k) \approx \delta k_x\sigma^y + (1/2(\delta k_x)^2 + 2\delta\kappa)\sigma^z \approx \delta k_x\sigma^x + m(\delta\kappa)\sigma^z \quad (3)$$

where the mass function $m(\delta\kappa) \equiv 2\delta\kappa$, and nothing depends on θ. Thus, near the Fermi surface we find a family of 1D Dirac Hamiltonians along the x-direction with masses depending on the radius in k-space away from the Fermi-surface ($\delta\kappa$) in the $k_y k_z$-plane which can be positive or negative. This expansion shows that at each (k_y, k_z) we have the Hamiltonian of a massive 1D Dirac model, and the sign of the mass (and thus topological phase) changes as a function of (k_y, k_z) as one passes through the FL. This validates our perspective of a LTSM

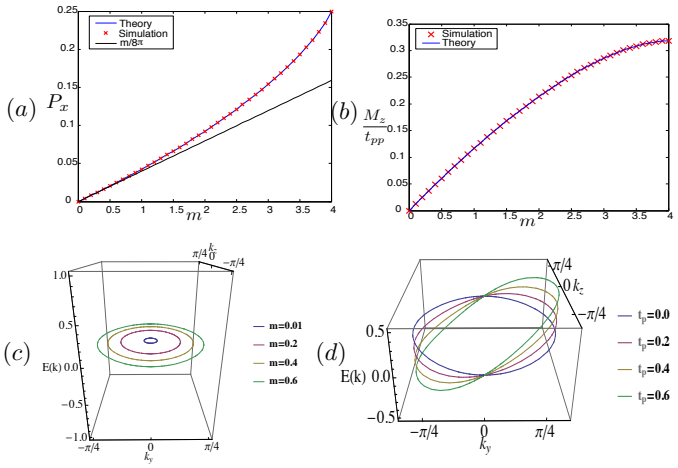

FIG. 1. (a) The polarization for the model in Eq. 2 is plotted vs. the parameter m in the model with $\beta = \gamma = 2$. (b) The magnetization for the model in Eq. 2 with the extra term $t_{pp} \sin k_y \mathbb{I}$ is plotted vs various values of m for $\beta = \gamma = 2$. (c) The location of the line node is plotted in the $E - k_y - k_z$ space with $k_x = 0$ for $t_{pp} = 0$ and various values of m with $\beta = \gamma = 2$. The polarization is proportional to the area enclosed by the FL. (d) The location of the line node is plotted in the $E - k_y - k_z$ space with $k_x = 0$ for $m = 1$ and various values of t_{pp} with $\beta = \gamma = 2$. The magnetization is proportional to integral of the energy around the FL in momentum space.

as a collection of 1D wires where the FL represents the topological phase transition between contiguous regions of wires in the BZ. We expect the low-energy Hamiltonian near any non-degenerate FL to take a similar form, regardless of the microscopic lattice model from which it emerges. One immediate conclusion we can draw from this analysis is that this model will have a surface charge from the localized topological modes at the ends of the wires in the topological region in momentum space, i.e., the region either inside or outside the FL. Below we will explicitly show that this surface charge is a consequence of a bulk polarization, and also that this model has the EM response Eq. 1 with $\mathcal{B}_{yz} \neq 0$.

Now, let us step away from our example model and generically determine the polarization of a LTSM in some fixed direction $\hat{n}$. It is useful to treat our 3D Bloch Hamiltonian as a family of 1D Bloch Hamiltonians $H_{\vec{k}_\perp}(k_\parallel)$ parameterized by $\vec{k}_\perp, k_\parallel$, which are the components of the momentum perpendicular and parallel to $\hat{n}$. Generically, the family $H_{\vec{k}_\perp}(k_\parallel)$ is a set of 1D gapped Bloch Hamiltonians except when the point $(k_\parallel, \vec{k}_\perp)$ lies on one of the FLs (which only occupy a set of measure zero in the 3D BZ). Note that while the FLs in our model are planar, our results below apply to non-planar cases as well. To calculate the charge polarization we first need to first calculate the quantity[45]

$$\Theta_\parallel(\vec{k}_\perp) = \frac{e}{2\pi} \int dk_\parallel \mathrm{Tr}\left[\mathcal{A}_\parallel(k_\parallel, \vec{k}_\perp)\right] \tag{4}$$

where $\mathcal{A}_\parallel$ is the component of the Berry connection along $\hat{n}$. Let us first consider a special case where we evaluate $\Theta(\vec{k}_\perp)$ at $\vec{k}_\perp = \vec{\Lambda}_a$, where $\vec{\Lambda}_a$ is any inversion-invariant momentum in the $\vec{k}_\perp$ plane, i.e., $\vec{\Lambda}_a = -\vec{\Lambda}_a \mod \vec{G}$. Then $\Theta(\vec{\Lambda}_a)$ is quantized to be 0 or $e/2 \mod e$, if $H_{\vec{\Lambda}_a}(k_\parallel)$ is gapped, since this 1D Bloch Hamiltonian has inversion symmetry. We then consider a deviation away from $\vec{k}_\perp = \Lambda_a$ which is still in the plane normal to $\hat{n}$, and such that the Hamiltonian $H_{\vec{\Lambda}_a + \delta\vec{k}_\perp}(k_\parallel)$ is gapped. However, this 1D Bloch Hamiltonian does not have to be inversion invariant, and thus it is not immediately obvious how to evaluate $\Theta_\parallel$. However, we can use the following general argument to simplify the calculation. Let us evaluate the difference in the 1D polarizations

$$\Delta\Theta_\parallel = \quad \Theta_\parallel(\vec{\Lambda}_a + \delta\vec{k}_\perp) - \Theta_\parallel(\vec{\Lambda}_a) = \frac{e}{2\pi} \int_S \mathrm{Tr}\,[F] \tag{5}$$

where the last expression is a surface integral of the Berry curvature 2-form F over the region S bounded by the two closed circles located at $\vec{\Lambda}_a$ and $\vec{\Lambda}_a + \delta\vec{k}_\perp$, and spanned by $k_\parallel$ through the cycle of the BZ in the $\hat{n}$ direction. Crucially, since our system has $\mathcal{TI}$ symmetry, the only sources of Berry curvature are the π-flux lines carried by the FLs. Thus, generically $\Delta\Theta_\parallel$ itself is quantized to be either 0 or $\frac{e}{2} \mod e$ depending on the parity of the number of Dirac line-nodes enclosed in the surface S. The quantization of $\Delta\Theta_\parallel$ is completely general and does not rely on starting at an inversion-invariant momentum, it only relies on the existence of $\mathcal{TI}$ symmetry. The ability to start at an inversion-invariant momentum just informs us that the global constant needed to determine the full $\Theta_\parallel(\vec{k}_\perp)$ from the knowledge of only the $\Delta\Theta_\parallel(\vec{k}_\perp)$ is either 0 or $\frac{e}{2}$; data which is ultimately encoded in the secondary weak invariant ν_{ij} of the occupied bands.

For a system with a single FL we see that $\mathcal{B}_{ij}$, and hence, the overall charge polarization is simply proportional to the projected area of the FL in the $\hat{n}$ boundary BZ, i.e.,

$$e\mathcal{B}_{ij} \equiv 4\pi^2 \epsilon^{\hat{n}ij} P_{\hat{n}} = \int_{\perp BZ} d\vec{k}_\perp \Theta_\parallel(\vec{k}_\perp) = (-1)^{\nu_{ij}} \frac{e}{2} \Xi\, \Omega_{ij} \tag{6}$$

where Ω_{ij} is the area of the FL projected onto the ij-plane of the boundary BZ, $\Xi = \chi(\mathrm{sgn}\, m_{\mathcal{I}})$, $\chi = \pm 1$ corresponds to the FL helicity, i.e., the clockwise/counterclockwise flow of the Berry flux along the FL with respect to the normal $\hat{n}$, and ν_{ij} is the secondary weak invariant defined as the holonomy of the Berry gauge field of the occupied bands along the line $k_i = k_j = \pi$. This is a bulk calculation for the polarization, and only holds up to the addition of a quantum

of polarization[45]. Also, changing the secondary weak invariant ν_{ij}, can change the polarization by a quantum, and/or a sign, since it can switch the projected area to its complement in the surface BZ. For a single FL this effect is already taken into account in Eq. 6. However, for more than one FL, the bulk calculation will result in the sum of the projected areas of all the FLs modulo regions where an even number of FLs have overlapping projections. As shown in Appendix A, when FLs have overlapping projected areas, the connection between the bulk result and the surface charge requires some knowledge of the filling of the boundary states[25, 46].

One corollary of these general arguments is that, while it is not forbidden to have just a single closed FL in systems with $\mathcal{TI}$ symmetry, it is forbidden to have only one FL (or an odd number) which traverses a non-trivial cycle of the BZ and meets itself. We can see this because calculating any component of the polarization would indicate that the polarization must jump on either side of the FL, however this is not compatible with the periodicity of the BZ, and thus must be forbidden. This is a 3D line-node generalization of the fermion doubling theorem for Dirac nodes in 2D with $\mathcal{TI}$ symmetry.

To illustrate these results with our example model we calculate the polarization numerically in Fig. 1a where P_x of $H_3(k)$ is plotted vs. m with the corresponding geometry of the FL shown in Fig. 1c. We choose $\beta, \gamma = 2$ so that there is a single FL in the $k_x = 0$ plane and centered around the origin of the BZ. P_x should be proportional to the area enclosed by the FL given by $\cos k_y + \cos k_z = 2 - m/2$. For small values of m, the FL is approximately a circle of radius $\sqrt{m}$ and $P_x \approx \operatorname{sgn} m_{\mathcal{I}} \frac{m}{8\pi}$. This approximation works well when m is small, but underestimates P_x as m is increased. At $m = 4$, the FL given by $\cos k_y + \cos k_z = 0$ will enclose half the area of the BZ. The polarization has the symmetry $P_x(m) = \frac{e}{2} - P_x(8 - m)$ since for $m > 4$, the FL is just centered around $(k_y, k_z) = (\pi, \pi)$ on the boundary BZ instead of $(0, 0)$. Hence, we only show $0 \leq m \leq 4$ in Fig. 1a.

Now let us move on to studying the contributions of $\mathcal{B}_{0i}$ to the EM response. Similar to the 2D Dirac TSMs, which have a non-vanishing orbital magnetization when there is an energy difference between the Dirac nodes, LTSMs can also have a magnetization that depends on how the band touching lines are embedded in energy/momentum space. To produce this effect in our model, we need to change the energy along the nodal submanifold while preserving $\mathcal{TI}$, and we can do this, e.g., by adding an extra kinetic energy term $\epsilon(\vec{k})\mathbb{I}$ to $H_3(k)$. However, before calculating the result for our explicit model we will evaluate the magnetization in a generic system with $\mathcal{TI}$ symmetry.

Following Refs. 27 and 47, the orbital magnetization is given by

$$M^a = \frac{e\epsilon^{abc}}{2\hbar} \int \frac{d^d k}{(2\pi)^d} \sum_{\alpha=1}^{M} \operatorname{Im} \langle \partial_b \alpha | H(k) + \epsilon_\alpha(k) | \partial_c \alpha \rangle \tag{7}$$

where we have absorbed the dependence on the chemical potential μ into $H(k)$ and $\epsilon_\alpha(k)$, assumed M occupied bands, and a total of N bands with $M \leq N$. $\epsilon_\alpha(k)$ is the energy of the α-th band, and $|\alpha\rangle$ is shorthand notation for the Bloch state $|u_{\alpha,\mathbf{k}}\rangle$. This sum can be simplified as follows. First, consider the terms which depend on the band energies $\epsilon_\alpha(k)$ and rewrite them as

$$\sum_{\alpha=1}^{M} \operatorname{Im} \epsilon_\alpha(k) \langle \partial_b \alpha | \partial_c \alpha \rangle = \sum_{\alpha=1}^{M} \Big[\operatorname{Im} \epsilon_\alpha(k) \langle \partial_b \alpha | P_E(k) | \partial_c \alpha \rangle + \operatorname{Im} \epsilon_\alpha(k) \langle \partial_b \alpha | P_G(k) | \partial_c \alpha \rangle \Big],$$

where $P_E(k)$ and $P_G(k)$ are the projectors onto the unoccupied and occupied bands respectively at each value of k, and they satisfy $P_G(k) + P_E(k) = \mathbb{I}_{N \times N}$. Then, we see that the first term is related to the $U(M)$ Berry curvature of the occupied bands since $\epsilon_\alpha(k)$ is real-valued and[48]

$$\mathcal{F}_{bc}^{\alpha\alpha}(k) = \operatorname{Im} \left[\langle \partial_b \alpha | P_E(k) | \partial_c \alpha \rangle \right].$$

So, we have $\sum_{\alpha=1}^{M} \epsilon_\alpha(k) \mathcal{F}_{bc}^{\alpha\alpha}(k) + \sum_{\alpha=1}^{M} \operatorname{Im} \epsilon_\alpha(k) \langle \partial_b \alpha | P_G(k) | \partial_c \alpha \rangle$.

To simplify further let us consider the terms with $H(k)$. We can rewrite $H(k) = \sum_{\gamma=1}^{N} \epsilon_\gamma(k) |\gamma\rangle\langle\gamma|$. Then we have the sum $\sum_{\alpha=1}^{M} \sum_{\gamma=1}^{N} \operatorname{Im} \epsilon_\gamma(k) \langle \partial_b \alpha | \gamma \rangle \langle \gamma | \partial_c \alpha \rangle$. We note that $\langle \partial_b \alpha | \gamma \rangle = -\langle \alpha | \partial_b \gamma \rangle$. Using this on both of the matrix elements, we have $\sum_{\alpha=1}^{M} \sum_{\gamma=1}^{N} \operatorname{Im} \epsilon_\gamma(k) \langle \alpha | \partial_b \gamma \rangle \langle \partial_c \gamma | \alpha \rangle$. Now, we note that this is the same as $-\sum_{\alpha=1}^{M} \sum_{\gamma=1}^{N} \operatorname{Im} \epsilon_\gamma(k) \langle \partial_b \gamma | \alpha \rangle \langle \alpha | \partial_c \gamma \rangle$ with the overall minus sign coming from taking the complex conjugate. Next, the sum over α can be done to give us $P_G(k)$. So, we have $-\sum_{\gamma=1}^{N} \operatorname{Im} \epsilon_\gamma(k) \langle \partial_b \gamma | P_G(k) | \partial_c \gamma \rangle$.

Combining both sets of terms we find: $\sum_{\alpha=1}^{M} \epsilon_\alpha(k) \mathcal{F}_{bc}^{\alpha\alpha}(k) - \sum_{\beta=M+1}^{N} \epsilon_\beta(k) \overline{\mathcal{F}}_{bc}^{\beta\beta}(k)$ where we have used the fact that $\overline{\mathcal{F}}_{bc}^{\beta\beta}(k) = \operatorname{Im} \langle \partial_b \beta | P_G(k) | \partial_c \beta \rangle$ is the $U(N - M)$ Berry curvature of the unoccupied bands. So, the magnetization is given by:

$$M^a = \frac{e\epsilon^{abc}}{2\hbar} \int \frac{d^d k}{(2\pi)^d} \times \left(\sum_{\alpha=1}^{M} \epsilon_\alpha(k) \mathcal{F}_{bc}^{\alpha\alpha}(k) - \sum_{\beta=M+1}^{N} \epsilon_\beta(k) \overline{\mathcal{F}}_{bc}^{\beta\beta}(k) \right). \tag{8}$$

So far this expression is generic and does not use the $\mathcal{TI}$ symmetry that is present in the models we consider, but there is a key simplification in the Berry curvature

$\mathcal{F}^{\alpha\alpha}_{bc}(k)$ in the presence of this symmetry: $\mathcal{F}^{\alpha\alpha}_{bc}(k) = -\mathcal{F}^{\alpha\alpha}_{bc}(k)$[49]. Similarly, we have $\overline{\mathcal{F}}^{\beta\beta}_{bc}(k) = -\overline{\mathcal{F}}^{\beta\beta}_{bc}(k)$ under $\mathcal{TI}$. Thus, nominally the (diagonal matrix components) of the Berry curvature vanish everywhere in the Brillouin zone. However, as discussed earlier, stable band touchings can act as sources of quantized Berry curvature. For example, if bands α_1 and α_2 touch along a FL they will have $\mathcal{F}^{\alpha_1\alpha_1}_{bc} = -\mathcal{F}^{\alpha_2\alpha_2}_{bc} = \Xi\pi\delta(\mathbf{k}-\mathbf{k}_0)$ (recall $\Xi = \pm 1$). Bands can touch each other along FLs with a crossing which can be linear as we consider in this paper, quadratic or any higher order. The higher order band crossings will act as sources of Berry curvature with higher multiples of π, but they are not stable without the addition of more symmetries, and can be broken down to a number of linear crossings with the minimal, non-vanishing flux quantization. Bands which do not touch any other bands in the BZ, or touch along accidental crossings, will have vanishing Berry curvature at each point of the BZ and will not contribute to the magnetization. Since we are only interested in LTSMs we will not consider cases with point-like sources of Berry curvature coming, e.g., from Weyl or Dirac nodes, and instead only calculate the contributions from FLs.

Before we move on, we quote a technical result, derived in Appendix B, which is needed for further analysis:

$$\mathrm{Im}\,\langle\partial_b\alpha_1|\alpha_2\rangle\langle\alpha_2|\partial_c\alpha_1\rangle = -\mathrm{Im}\,\langle\partial_b\alpha_2|\alpha_1\rangle\langle\alpha_1|\partial_c\alpha_2\rangle$$

when $\mathcal{TI}$ symmetry is enforced. Hence $\mathrm{Im}\,\langle\partial_b\alpha_1|\alpha_2\rangle\langle\alpha_2|\partial_c\alpha_1\rangle = 0$ or $\pi\Xi\delta(k-k_0)$ when the α_1-th and α_2-th band either do not touch, or touch at k_0 respectively. If we consider the full non-abelian Berry curvature $\mathcal{F}^{\alpha\alpha}_{bc} = \sum_{\beta=M+1}^{N}\mathrm{Im}\,\langle\partial_b\alpha|\beta\rangle\langle\beta|\partial_c\alpha\rangle$, we see that terms involving bands $\beta \in M+1,\ldots,N$ that do not touch the α-th band along FLs drop out in the sum because they are zero. The ones that do touch satisfy the δ-function property. In the case that α touches a *single* band $\overline{\alpha}$ among the unoccupied bands along a FL, we have $\mathcal{F}^{\alpha\alpha}_{bc} = \pi\Xi\delta(k-k_{\alpha\bar{\alpha}})$ where $k_{\alpha\bar{\alpha}}$ is the location of the appropriate line node. This follows by looking at the only non-zero element in the sum and its properties under $\mathcal{TI}$. If we had more bands touching the α-th band along a nodal line, we have $\mathcal{F}^{\alpha\alpha}_{bc} = \sum_{\beta\,\text{touch}\,\alpha}\pi\Xi_{\alpha\beta}\delta(k-k_{\alpha\beta})$. Similar properties hold for those unoccupied bands which form the FLs with the occupied ones, i.e., $\overline{\mathcal{F}}^{\beta\beta}_{bc} = -\sum_{\alpha\,\text{touch}\,\beta}\pi\Xi_{\alpha\beta}\delta(k-k_{\alpha\beta})$.

In the magnetization integral, we have to integrate $\sum_{\alpha=1}^{M+1}\epsilon_\alpha\mathcal{F}^{\alpha\alpha}_{bc} - \sum_{\beta=M+1}^{N}\epsilon_\beta\overline{\mathcal{F}}^{\beta\beta}_{bc}$. For each δ-function in the first term, there is a corresponding δ-function in the second term with an opposing sign. Further, since the only contributions to the Berry curvature are at band touching points, the energies of the two bands must coincide $\epsilon_\alpha = \epsilon_{\overline{\alpha}}$. Crossings which are completely beneath the Fermi level do not contribute to the magnetization since they will cancel out in the sum over occupied bands from Eq. 8. Combining these results, we find that the quantity that needs to be integrated is $2\epsilon_\alpha\mathcal{F}^{\alpha\alpha}_{bc}$ for each band α that has a FL crossing the Fermi level. Thus, the expression for the magnetization can then be written as:

$$M^a = \sum_{\alpha\in\text{bands that cross at }\mu=0}\frac{e\epsilon^{abc}}{2\hbar}\int\frac{d^3k}{(2\pi)^3}2\epsilon_\alpha\mathcal{F}^{\alpha\alpha}_{bc} \tag{9}$$

$$= \sum_\alpha\frac{e}{4\pi\hbar}\int_{\partial R_\alpha}\epsilon_\alpha(\mathbf{k})\,dk^a \tag{10}$$

where ∂R_α denotes the location of the line-node arising from the α-th band in the BZ at the Fermi level; $\partial R_\alpha = \varnothing$ if there is no band crossing for the α-th band at the Fermi level. Our result now shows the appropriate generalization to FLs of the energy difference between point-nodes that was previously shown to contribute to the EM response Weyl and Dirac semimetals. Thus, for each FL we can define the mixed space and time components of the 2-form:

$$\mathcal{B}^{0a} = \frac{\pi\Xi}{\hbar}\int_{\partial R}\epsilon(\vec{k})dk^a = \frac{4\pi^2}{e}M^a \tag{11}$$

where the integration is over the nodal line. The total magnetization, and total 2-form, include a sum over all FLs that cross the Fermi-level. This is a 3D generalization of the results of Refs. 25 and 28 that relate the magnetization of the 2D Dirac semimetal to the energy differences between the band-touching points. As an explicit illustration, in Appendix B we calculate the magnetization for a generic two-band model and show that the results match our calculation.

One can give a microscopic argument for the existence of the magnetization/boundary currents for surfaces that harbor protected, low-energy modes. The surface states of $H_3(k)$ are initially flat-bands that do not disperse, and $\epsilon(k)$ will impart a dispersion as a function of (k_y, k_z). In general, this will create a bound surface current in the $y-z$ plane which is the consequence of a non-vanishing bulk magnetization density. There will be similar currents on surfaces without low-energy modes, but there is not as simple of an interpretation[25].

We confirm this result numerically by adding an extra term $t_{pp}\sin k_y\mathbb{I}$ to $H_3(k)$ and plotting the magnetization vs. m in Fig. 1b. The magnetization has the symmetry $M_z(m) = M_z(8-m)$, and we restrict ourselves to $0 \le m \le 4$ in Fig. 1b. The magnetization is given by $\frac{M^z(m)}{t_{pp}} = \mathrm{sgn}\,m_{\mathcal{I}}\frac{e}{4\pi\hbar}\int_{-k_0}^{k_0}\sin k_y\,dk_z$. Again we have fixed $\beta,\gamma = 2$ so that there is only one FL, which has $\chi = +1$. The magnetization for this case can also be evaluated analytically from Eq. 25 since the energy only depends on k_y. The limits to which k_z extends for the FL can be calculated using the equation for the nodal line $(\cos k_y + \cos k_z = 2 - m/2)$. Hence, on the nodal line, k_y is a function of k_z. The maximum value of $\cos k_y = 1$,

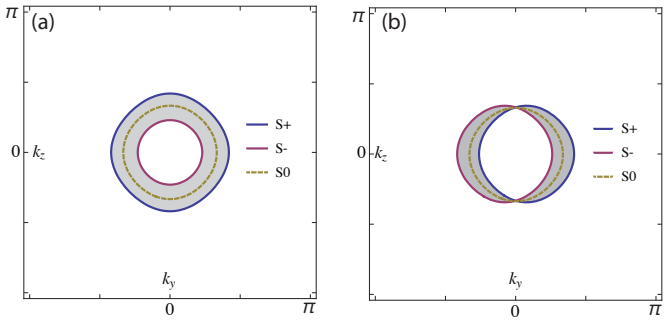

FIG. 2. Dotted yellow lines represent initial four-fold degenerate Fermi-line ($S0$). Purple and blue solid lines represent spin-split Fermi-surfaces ($S+, S-$) with (a) a majority and minority spin Fermi-line induced by certain $\mathcal{T}$-breaking terms (b) spin-split Fermi-lines with equal sizes for each spin reminiscent of a Rashba-type splitting from spin-orbit terms induced by strain/inversion breaking. For both panels the gray shaded region represents the magnitude of the polarization in the x-direction from the projected areas of the Fermi lines after Z_2 overlap cancellation.

and this means that the maximum/minimum k_z is given by $\pm k_{z0} = \pm\cos^{-1}(1 - m/2)$. This is valid only when $m < 4$, while for $m > 4$, the FL is centered around (π, π) instead of the origin. The magnetization is a function of m, and does not have a simple closed form expression. However, it does have a linear profile in the regime when m is small.

We have now completed our goal of showing that the LTSM EM response given by Eq. 1 can be related to the geometry of the line-nodes in energy momentum space. To conclude, we comment on the applicability of our results to real materials. The magnetic heterostructure proposed in Refs. 32 and 39 breaks $\mathcal{T}$ explicitly, hence the spins are not degenerate, and the line nodes occur with just two overlapping bands. Thus, this model corresponds precisely to an effectively spinless case that has been described throughout this paper, and our results can be directly applied. We expect, and have confirmed numerically, that this system will have a charge polarization. It is worth noting that the two form $\mathcal{B}_{\mu\nu}$ explicitly enters the continuum Hamiltonian of this system as, for example, $H = \vec{k}\cdot\vec{\Gamma} + i\mathcal{B}_{yz}\Gamma^0\Gamma^{yz}$ where Γ^μ are a set of Dirac matrices. One could pursue a continuum diagrammatic calculation of our result using this spinful system, but we will not do so in this paper. In the case of spin degenerate models, which are found, for example, in the carbon allotrope materials in Refs. 40 and 41, a further reflection symmetry is required to stabilize the LTSM arising from four overlapping bands as shown in Ref. 50. For doubly-degenerate bands the charge polarization, being a $\mathbb{Z}_2$ quantity, is trivial. However, we can break spin degeneracy by including certain $\mathcal{T}$-breaking terms, or inducing additional spin orbit terms via strain, with the requirement that the FLs are not completely destabilized to a gapped, or point-node, phase. If we take two copies of our model, one for each spin, then two illustrations of initially spin-degenerate FLs (in the $k_x = 0$ plane) split by two types of spin-dependent terms are shown in Fig. 2. In these cases, the polarization P_x can be nontrivial and is not completely $\mathbb{Z}_2$ canceled. In fact, in both cases, the shaded areas correspond to the magnitude of the polarization, assuming a vanishing secondary weak invariant. The magnetization, on the other hand, is not a $\mathbb{Z}_2$ quantity and can be non-vanishing even for four-fold degenerate FLs. Hence, we expect that these systems would exhibit charge polarization when the FLs are spin-split via strain or other spin-dependent perturbations.

We would like to thank P.Y. Chang, V.K. Chua, V. Dwivedi, and A. Tiwari for discussions. We acknowledge support from ONR YIP Award N00014-15-1-2383.

Appendix A: Multiple FLs and the polarization

When we have multiple FLs, the problem of calculating the polarization precisely is not quite as simple because the boundary charge is decided by the overlap and filling of the low energy boundary states that are enclosed by the multiple FLs. Despite this, even in the most general setting, the polarization can be written down as a signed-sum of the various projected areas enclosed by the various FLs. As described in the main text, we showed that we can perform a simple bulk calculation to determine a set of values for these signs. However, a precise surface theorem giving the bound charge associated to the polarization change at an interface is meaningful only when the occupations of the surface states are specified (similar to the complications in Refs. 25 and 46 for the polarizations in a Chern insulator or 2D Dirac semi-metal respectively). If the boundary occupations are precisely known, then one can determine the necessary sign for each area contribution that will determine the correct surface charge. Hence, the projected areas that determine the surface charge are decided by the geometry of the FLs, but the signs multiplying each area can differ from the bulk calculation, and depend explicitly on the boundary state occupation.

The results simplify when there is only one or two FLs in the system. In the former case, the surface charge is determined (up to a sign decided by the inversion-symmetry breaking) by whether the surface states exist inside or outside the FL. For two (or more) FLs another complication appears due to the possibility of the projected areas overlapping in the surface BZ. In these cases we can have edge states overlapping, and we expect generically that a $\mathbb{Z}_2$ cancelation will occur for the overlapping states. Now, let us show how we can determine the bulk value of the polarization precisely for the case of two line nodes. A natural guess for a generalization of the polarization formula we have derived in Eq. 6 would

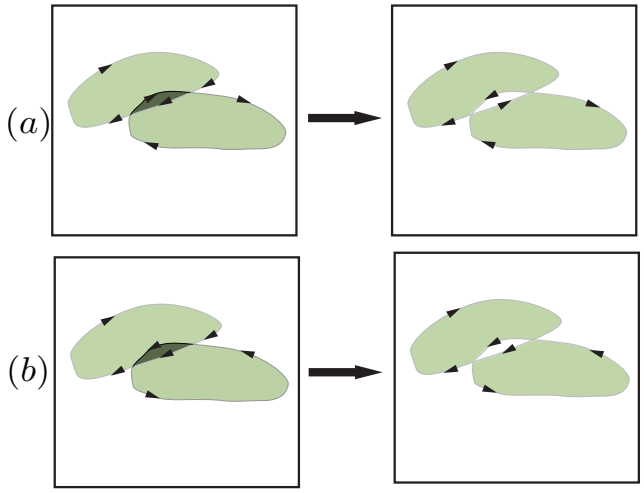

FIG. 3. Rules for the modification of $\chi \mathrm{sgn}\, m_{\mathcal{I}}$ for the determination of the boundary charge for the case of two FLs are illustrated. The green shaded areas represent regions where edge states exist, and the dark green area represents areas where there are overlapping edge states. Case (a) needs a reassignment of arrows while case (b) does not.

be

$$P^i = \epsilon^{ijk}(-1)^{\nu_{jk}} \sum_a \frac{e}{8\pi^2} \Xi_a \Omega_{a,jk}, \tag{12}$$

but this unfortunately does not account for the possible $\mathbb{Z}_2$ cancelations. To account for this we start off by drawing the projected FLs in the appropriate surface BZ perpendicular to the polarization direction. We must take care to include arrows indicating the direction along which Berry flux is flowing along the FL with respect to the surface normal. The flow is clockwise when the product $\chi \mathrm{sgn}\, m_{\mathcal{I}} = +1$ and counterclockwise for the product $\chi \mathrm{sgn}\, m_{\mathcal{I}} = -1$ where χ corresponds to the FL helicity with respect to the normal along the ith direction. If there are some regions where the projected areas of the FLs overlap, we have to carefully handle the $\mathbb{Z}_2$ cancellation. We assume that any place where two FL areas overlap there is a cancellation. We can effectively take this into account in our formula after performing a simple graphical analysis. First, if the weak invariant $(-1)^{\nu_{ij}} = -1$, we start off by shading the region around (π, π), else we leave it unshaded. Then every time we cross a FL, we change from shaded to unshaded and vice versa. This prescription gives us a unique way of shading the entire surface BZ with the projected FLs where *alternating* regions are shaded. The shaded regions naturally represent regions of the surface BZ with stable surface states. After we are done with shading, we check if the regions which are shaded have an arrow consistently going clockwise/counterclockwise on its boundary. If they do, we sum over the areas of the regions shaded with the product $\chi \mathrm{sgn}\, m_{\mathcal{I}}$ for that region coming from the direction of the arrow on the boundary. If the direction of arrows is inconsistent, we follow the reassignment of the arrows as shown in Fig. 3 and sum over the modified areas.

With more FLs, this prescription does not give us a unique answer in regions which have *more* than two sets of edge states overlapping. The sign of the polarization arising from these regions depends on the details of how the surface states are coupled to give the $\mathbb{Z}_2$ cancelation, and hence how the states are occupied. The value of the polarization that matches the surface charge is ultimately still a signed sum of the projected areas, but these signs can only be determined after the occupation of the edge state branches is chosen. All of these issues arise due to the $\mathbb{Z}_2$ stability of the edge states, as opposed to the $\mathbb{Z}$ stable chiral case. We will leave the problem of exhaustive treatment of generic FL configurations to future work.

Appendix B: $\mathcal{TI}$ symmetry and Berry curvatures

To prove the result about the properties of the Berry curvature for a line-node, we switch back to writing out the ket $|\alpha\rangle = u_{\alpha,\mathbf{k}}$ as a column vector with u^i_α being the ith component (the bras will be row vectors and we will use lowered indices for them). Let us consider the following matrix element $M = \mathrm{Im}\,\langle \partial_b \alpha_1 | \alpha_2 \rangle \langle \alpha_2 | \partial_c \alpha_1 \rangle = \mathrm{Im}\,(\partial_b u^*_{\alpha_1,i}) u^i_{\alpha_2} u^*_{\alpha_2,j} (\partial_c u^j_{\alpha_1})$ and its transformation properties under $\mathcal{TI}$, where we assume that $\mathcal{TI} = UK$ with U being a constant unitary matrix. Repeated indices of i, j, k are assumed to be summed. The action of $\mathcal{TI}$ on the matrix element gives us the following:

$$\begin{aligned} M &= \mathrm{Im}\,((U^\dagger)^k_i \partial_b u_{\alpha_1,k})(U^i_r u^{r,*}_{\alpha_2})((U^\dagger)^s_j u_{\alpha_2,s})(U^j_p \partial_c u^{p,*}_{\alpha_1}) \\ &= \mathrm{Im}\,(\partial_b u_{\alpha_1,k})(u^{k,*}_{\alpha_2})(u_{\alpha_2,s})(\partial_c u^{s,*}_{\alpha_1}) \\ &= -\mathrm{Im}\,(\partial_b u^*_{\alpha_1,i}) u^i_{\alpha_2} u^*_{\alpha_2,j} (\partial_c u^j_{\alpha_1}) \end{aligned} \tag{13}$$

where the asterisk denotes complex conjugation. We have summed over i, j when we go from the first to the second line to get rid of factors of U. The minus sign from the second to the third line comes from conjugation. Further, we have used the following symmetry properties of the Bloch states under $\mathcal{TI}$ given by:

$$u^i_\alpha = U^i_j u^j_\alpha,\ u^*_{\alpha,i} = (U^\dagger)^j_i u^*_{\alpha,j} \tag{14}$$

Put together, what we have proved is that $\mathrm{Im}\,\langle \partial_b \alpha_1 | \alpha_2 \rangle \langle \alpha_2 | \partial_c \alpha_1 \rangle = -\mathrm{Im}\,\langle \partial_b \alpha_1 | \alpha_2 \rangle \langle \alpha_2 | \partial_c \alpha_1 \rangle$ under $\mathcal{TI}$. We also note that $\mathrm{Im}\,\langle \partial_b \alpha_1 | \alpha_2 \rangle \langle \alpha_2 | \partial_c \alpha_1 \rangle = \mathcal{F}^{\alpha_1 \alpha_1}_{bc,proj}$ is the Berry curvature of the α_1th band coming from the Hamiltonian $H_{12} = \epsilon_{\alpha_2} |\alpha_2\rangle\langle\alpha_2| + \epsilon_{\alpha_1} |\alpha_1\rangle\langle\alpha_1|$ (We call this the projected α_1, α_2 subsystem). What we have proved with our analysis of the matrix element under $\mathcal{TI}$ is that $\mathcal{F}^{\alpha_1 \alpha_1}_{bc,proj} = -\mathcal{F}^{\alpha_1 \alpha_1}_{bc,proj} \bmod 2\pi$. If the two bands do not cross, clearly the projected Berry curvature should

be zero at every point in the BZ. If on the other hand, they do touch along stable FLs we can see that it must be equal to $\pi\Xi\delta(k-k_0)$ where k_0 is the location of the nodal line. The other identity which we use is that $\mathrm{Im}\,\langle\partial_b\alpha_1|\alpha_2\rangle\langle\alpha_2|\partial_c\alpha_1\rangle = -\mathrm{Im}\,\langle\partial_b\alpha_2|\alpha_1\rangle\langle\alpha_1|\partial_c\alpha_2\rangle$, i.e. $\mathcal{F}^{\alpha_1\alpha_1}_{bc,proj} = -\mathcal{F}^{\alpha_2\alpha_2}_{bc,proj}$ in the projected system. This simply follows from the property that $\langle\alpha_2|\partial_a\alpha_1\rangle = -\langle\partial_a\alpha_2|\alpha_1\rangle$. Thus, we must have:

$$\begin{aligned}\mathrm{Im}\,\langle\partial_b\alpha_1|\alpha_2\rangle\langle\alpha_2|\partial_c\alpha_1\rangle &= \mathrm{Im}\,\langle\alpha_1|\partial_b\alpha_2\rangle\langle\partial_c\alpha_2|\alpha_1\rangle \\ &= \mathrm{Im}\,(\langle\partial_b\alpha_2|\alpha_1\rangle\langle\alpha_1|\partial_c\alpha_2\rangle)^* \\ &= -\mathrm{Im}\,\langle\partial_b\alpha_2|\alpha_1\rangle\langle\alpha_1|\partial_c\alpha_2\rangle \quad (15)\end{aligned}$$

as claimed.

Appendix C: Magnetization in a LTSM Model

Let us now calculate the magnetization for our model, which will eventually give us insight into the generic form for all LTSMs. The calculation of the (orbital) magnetization in crystalline systems was developed in Refs. 27 and 47, and the result of our calculation is essentially an extension of the results of the 2D Dirac semimetal shown in Refs. 25 and 28. To proceed, the adiabatic (Berry) curvatures $\mathcal{F}_{xy}, \mathcal{F}_{yz}, \mathcal{F}_{zx}$ for the following generic two-band model are calculated:

$$H(k) = A(\vec{k})\sigma^x + m_{\mathcal{I}}\sigma^y + B(\vec{k})\sigma^z \quad (16)$$

where $m_{\mathcal{I}}$ represents an infinitesimal inversion-breaking mass term that must be added to properly calculate the magnetization. Note that for the purposes of calculating the adiabatic curvatures, the additional $\epsilon(\vec{k})\mathbb{I}$ term that we will add to change the energy of the FL can be ignored since its inclusion will not affect the Bloch wavefunctions. The adiabatic curvature can be represented by defining the unit vector $\hat{d}$ as

$$\hat{d}(\vec{k}) = \frac{(A, m_{\mathcal{I}}, B)}{\sqrt{A^2 + m_{\mathcal{I}}^2 + B^2}} \quad (17)$$

which yields

$$\mathcal{F}_{ij} = \epsilon^{abc}\hat{d}_a\partial_i\hat{d}_b\partial_j\hat{d}_c \quad (18)$$

where $\partial_i = \frac{\partial}{\partial k_i}$ for $i = x, y, z$. So for the model in Eq. 16 we have

$$\mathcal{F}_{ij} = m_{\mathcal{I}}\frac{\partial_i A\,\partial_j B - \partial_j A\,\partial_i B}{(A^2 + m_{\mathcal{I}}^2 + B^2)^{3/2}}. \quad (19)$$

For the case of the semimetal, the limit of $m_{\mathcal{I}} \to 0$ must be taken. Using the identity that $\lim_{\epsilon\to 0}\frac{\epsilon}{\epsilon^2+\alpha^2} = \pi\,\mathrm{sgn}\,m_{\mathcal{I}}\,\delta(\alpha)$, the curvature can be simplified to

$$\mathcal{F}_{ij} = \pi\,\mathrm{sgn}\,m_{\mathcal{I}}\delta(\sqrt{A^2+B^2})\frac{\partial_i A\,\partial_j B - \partial_j A\,\partial_i B}{\sqrt{A^2+B^2}}. \quad (20)$$

If we think about the actual terms $A(\vec{k})$ and $B(\vec{k})$ from the model H_3, then we quickly see that the δ-function only has non-zero support exactly on the line-nodes. Generically, when $A(\vec{k})$ and $B(\vec{k})$ both vanish, then the system is gapless (when $m_{\mathcal{I}} \to 0$), and these gapless regions are the only sources of adiabatic curvature for a system with $\mathcal{TI}$ symmetry. Thus, in the gapless, semimetallic limit the only adiabatic curvature in the BZ is localized exactly on the FL, which we know must be the case for a model with $\mathcal{TI}$ symmetry.

To finish the magnetization calculation, consider the model $\bar{H}_3(\vec{k}) = \epsilon(\vec{k})\mathbb{I} + H_3(\vec{k})$ which now has broken $\mathcal{T}$ and broken $\mathcal{I}$, but preserves $\mathcal{TI}$. The expression for the magnetization density in terms of Bloch bands is given by[47]

$$M^a = \epsilon^{abc}\frac{e}{2\hbar}\int\frac{d^3k}{(2\pi)^3}\mathrm{Im}\langle\partial_b u_-|(\bar{H}_3(k) + E_-(k))|\partial_c u_-\rangle \quad (21)$$

where $E_-(k), |u_-\rangle$ are the energy and Bloch functions of the lower occupied band, and the derivatives are with respect to momentum. From symmetry, and from the fact that the extra kinetic term is proportional to the identity matrix, the above expression simplifies to

$$M^a = \mathrm{sgn}\,m_{\mathcal{I}}\frac{e\epsilon^{abc}}{4\hbar}\int_{BZ}\frac{d^3k}{(2\pi)^3}2\epsilon(\vec{k})\mathcal{F}_{bc}. \quad (22)$$

The expression from Eq. 20 for the curvature can now be substituted. Notice that we can do a coordinate transformation under the integral from $(k_a, k_b, k_c) \to (k_a, A, B)$ and the Jacobian of the transformation $J = |\partial_i A\partial_j B - \partial_j A\partial_i B|$ is already sitting in the curvature up to a total sign. Using the property that $\int_{\mathbf{X}}\delta(g(x))f(g(x))|g'(x)|dx = \int_{g(\mathbf{X})}\delta(u)f(u)du$, we can rewrite Eq. 22 as

$$M^a = \pm\,\mathrm{sgn}\,m_{\mathcal{I}}\frac{e}{4\hbar}\int\frac{dk^a dA dB}{(2\pi)^2}2\epsilon(\vec{k})\frac{\delta(\sqrt{A^2+B^2})}{\sqrt{A^2+B^2}} \quad (23)$$

where the domain of integration has now changed to the range of values which A, B take over the BZ and the outer signs represent the helicity of the FL, i.e. the sign of the Jacobian. We can make a coordinate transformation to polar coordinates in $A, B \to r, \theta$ where we note that r, θ could in general depend on k^a.

$$M^a = \pm\,\mathrm{sgn}\,m_{\mathcal{I}}\frac{e}{4\hbar}\int\frac{dk^a \times r dr d\theta}{(2\pi)^2}2\epsilon(\vec{k})\frac{\delta(r)}{r} \quad (24)$$

which can be simplified by integrating the expressions over r, θ. The δ function localizes the integral to the FL and the integral over θ gives us a factor of 2π.

$$\vec{M} = \pm\,\mathrm{sgn}\,m_{\mathcal{I}}\frac{e}{4\pi\hbar}\int_{\partial R}\epsilon(\vec{k})d\vec{k} \quad (25)$$

where we have explicitly indicated that the integration in Eq. 25 is over the FL which is equivalent to ∂R. We note that the magnetization results from integrating the energy of each point on the FL along the line node. Again, the $\pm$ sign in front of the magnetization tells us the sense in which the Berry flux circulates along the string, i.e., clockwise or counter-clockwise. This is a simple derivation of the bulk magnetization in the case of a single line node. If there are multiple FLs, contributions to the magnetization from each FL using Eq. 25 must be added up, but the result is not as complicated as the polarization with multiple FLs since the magnetization adds up normally, not as a Z_2 quantity. It is important to note that the connection between the bulk magnetization calculation and the boundary current can depend on the details of how the boundary states are filled similar to what was shown in Refs. 25 for 2D Dirac semi-metals.

[1] M. Z. Hasan and C. L. Kane, Rev. Mod. Phys. **82**, 3045 (2010).
[2] B. A. Bernevig, *Topological Insulators and Topological Superconductors* (Princeton University Press, 2013).
[3] F. Haldane, Phys. Rev. Lett. **61**, 2015 (1988).
[4] X.-L. Qi, T. L. Hughes, and S.-C. Zhang, Phys. Rev. B **78**, 195424 (2008).
[5] A. P. Schnyder, S. Ryu, A. Furusaki, and A. W. Ludwig, Phys. Rev. B **78**, 195125 (2008).
[6] A. Kitaev, arXiv preprint arXiv:0901.2686 (2009).
[7] L. Fu and C. L. Kane, Phys. Rev. B **76**, 045302 (2007).
[8] J. C. Y. Teo, L. Fu, and C. L. Kane, Phys. Rev. B **78**, 045426 (2008).
[9] L. Fu, Phys. Rev. Lett. **106**, 106802 (2011).
[10] T. L. Hughes, E. Prodan, and B. A. Bernevig, Phys. Rev. B **83**, 245132 (2011).
[11] D. Hsieh, D. Qian, L. Wray, Y. Xia, Y. S. Hor, R. J. Cava, and M. Z. Hasan, Nature **452**, 970 (2008).
[12] J. Moore, Nat. Phys. **5**, 378 (2009).
[13] Y. Xia, D. Qian, D. Hsieh, L. Wray, A. Pal, H. Lin, A. Bansil, D. Grauer, Y. Hor, R. Cava, *et al.*, Nat. Phys. **5**, 398 (2009).
[14] T. Zhang, P. Cheng, X. Chen, J.-F. Jia, X. Ma, K. He, L. Wang, H. Zhang, X. Dai, Z. Fang, *et al.*, Phys. Rev. Lett. **103**, 266803 (2009).
[15] C. L. Kane and E. J. Mele, Phys. Rev. Lett. **95**, 226801 (2005).
[16] B. A. Bernevig, T. L. Hughes, and S.-C. Zhang, Science **314**, 1757 (2006).
[17] M. König, H. Buhmann, L. W. Molenkamp, T. Hughes, C.-X. Liu, X.-L. Qi, and S.-C. Zhang, Journal of the Physical Society of Japan **77** (2008).
[18] C.-Z. Chang, J. Zhang, X. Feng, J. Shen, Z. Zhang, M. Guo, K. Li, Y. Ou, P. Wei, L.-L. Wang, *et al.*, Science **340**, 167 (2013).
[19] S.-Y. Xu, C. Liu, N. Alidoust, M. Neupane, D. Qian, I. Belopolski, J. Denlinger, Y. Wang, H. Lin, L. Wray, *et al.*, Nat. Comm. **3**, 1192 (2012).
[20] Y. Tanaka, Z. Ren, T. Sato, K. Nakayama, S. Souma, T. Takahashi, K. Segawa, and Y. Ando, Nat. Phys. **8**, 800 (2012).
[21] A. H. Castro Neto, F. Guinea, N. M. R. Peres, K. S. Novoselov, and A. K. Geim, Rev. Mod. Phys. **81**, 109 (2009).
[22] X. Wan, A. M. Turner, A. Vishwanath, and S. Y. Savrasov, Phys. Rev. B **83**, 205101 (2011).
[23] S. M. Young, S. Zaheer, J. C. Y. Teo, C. L. Kane, E. J. Mele, and A. M. Rappe, Phys. Rev. Lett. **108**, 140405 (2012).
[24] Z. Wang, Y. Sun, X.-Q. Chen, C. Franchini, G. Xu, H. Weng, X. Dai, and Z. Fang, Phys. Rev. B **85**, 195320 (2012).
[25] S. T. Ramamurthy and T. L. Hughes, Phys. Rev. B **92**, 085105 (2015).
[26] H. B. Nielsen and M. Ninomiya, Physics Letters B **105**, 219 (1981).
[27] J. Shi, G. Vignale, D. Xiao, and Q. Niu, Physical review letters **99**, 197202 (2007).
[28] D. Xiao, W. Yao, and Q. Niu, Phys. Rev. Lett. **99**, 236809 (2007).
[29] A. Zyuzin and A. Burkov, Phys. Rev. B **86**, 115133 (2012).
[30] Y. Ran, arXiv preprint arXiv:1006.5454 (2010).
[31] T. L. Hughes, H. Yao, and X.-L. Qi, arXiv preprint arXiv:1303.1539 (2013).
[32] A. A. Burkov, M. D. Hook, and L. Balents, Phys. Rev. B **84**, 235126 (2011).
[33] G. Bian, T.-R. Chang, R. Sankar, S.-Y. Xu, H. Zheng, T. Neupert, C.-K. Chiu, S.-M. Huang, G. Chang, I. Belopolski, *et al.*, Nature communications **7** (2016).
[34] G. Bian, T.-R. Chang, H. Zheng, S. Velury, S.-Y. Xu, T. Neupert, C.-K. Chiu, S.-M. Huang, D. S. Sanchez, I. Belopolski, *et al.*, Physical Review B **93**, 121113 (2016).
[35] M. Neupane, I. Belopolski, M. M. Hosen, D. S. Sanchez, R. Sankar, M. Szlawska, S.-Y. Xu, K. Dimitri, N. Dhakal, P. Maldonado, *et al.*, Phys. Rev. B **93**, 201104 (2016).
[36] S. S. Pershoguba and V. M. Yakovenko, Phys. Rev. B **86**, 075304 (2012).
[37] P.-Y. Chang, S. Matsuura, A. P. Schnyder, and S. Ryu, arXiv preprint arXiv:1406.0232 (2014).
[38] S. Matsuura, P.-Y. Chang, A. P. Schnyder, and S. Ryu, New Journal of Physics **15**, 065001 (2013).
[39] M. Phillips and V. Aji, Physical Review B **90**, 115111 (2014).
[40] K. Mullen, B. Uchoa, and D. T. Glatzhofer, arXiv preprint arXiv:1408.5522 (2014).
[41] H. Weng, Y. Liang, Q. Xu, Y. Rui, Z. Fang, X. Dai, and Y. Kawazoe, arXiv preprint arXiv:1411.2175 (2014).
[42] Y. Kim, B. J. Wieder, C. L. Kane, and A. M. Rappe, Phys. Rev. Lett. **115**, 036806 (2015).
[43] R. Yu, H. Weng, Z. Fang, X. Dai, and X. Hu, Phys. Rev. Lett. **115**, 036807 (2015).
[44] J. Zak, Phys. Rev. Lett. **62**, 2747 (1989).
[45] R. King-Smith and D. Vanderbilt, Phys. Rev. B **47**, 1651 (1993).
[46] S. Coh and D. Vanderbilt, Phys. Rev. Lett. **102**, 107603 (2009).
[47] D. Ceresoli, T. Thonhauser, D. Vanderbilt, and R. Resta, Phys. Rev. B **74**, 024408 (2006).
[48] X.-L. Qi, T. L. Hughes, and S.-C. Zhang, Phys. Rev. B **78**, 195424 (2008).
[49] F. D. M. Haldane, Phys. Rev. Lett. **93**, 206602 (2004).
[50] C. Fang, Y. Chen, H.-Y. Kee, and L. Fu, arXiv preprint arXiv:1506.03449 (2015).